DYNAMIC HORIZONTAL LOAD TESTS ON STEEL PIPE PILES HAVING DIFFERENT SIZES IN THE SAME CONSTRUCTION SITE AND THEIR ANALYSES

Eiji Kojima, Japan Pile Corporation, Tokyo, Japan
Hiromichi Kumagai, Japan Pile Corporation, Tokyo, Japan
Pastsakorn Kitiyodom, Kanazawa University, Kanazawa, Japan
Tatsunori Matsumoto, Kanazawa University, Kanazawa, Japan
Kouichi Tomisawa, Civil Engineering Research Institute of Hokkaido, Hokkaido, Japan

In this research, dynamic and static load tests were performed on permanent foundation piles which had a pile length of 30 m, 800 mm in outer diameter and 15 mm in wall thickness. In this site the dynamic horizontal load test on a smaller test pile, 12 m in length, 500 mm in outer diameter and 12 mm in wall thickness, was also carried out. The static horizontal load versus horizontal displacement derived from the dynamic load test conformed well to that measured in the conventional static horizontal load test of the pile with 800 mm diameter. Then an attempt was made to predict the horizontal load displacement of the pile with 800 mm diameter based on the results of the dynamic horizontal load test of the pile with smaller diameter of 500 mm.

INTRODUCTION

The design methods of foundation structures have been changing from allowable stress design to limit state design or performance based design in Japan after the Kobe Earthquake in 1995. Precise estimation of deformation of a pile foundation is a vital issue in the framework of these new design criteria. The simplest way to obtain the load-displacement relationship of a pile is to conduct an in-situ pile load testing. Many forms of pile load testing are conducted in practice.

For axial compressive pile load test methods, the dynamic load testing or the rapid load testing is widely used in Japan because of the fact that these methods are unsusceptible to reaction piles, and require less time and cost compared with the conventional static load test where reaction piles are employed. Application of the dynamic or rapid pile load test to horizontal pile load test would be very useful, although these test methods have not been specified in Japan.

In Kitiyodom et al. (2006), the possibility of the use of dynamic horizontal pile load test as an alternative method for the conventional static horizontal load testing is presented.

In actual construction sites, sometimes pile load tests to failure are not allowed for foundation piles are not allowed. Moreover, the use of an additional test pile having the same dimensions as the actual pile is difficult from an economical reason and so on. In that case, it may be useful to predict the load displacement of the actual pile from the load test of a smaller diameter test pile located near the actual pile.

In this work, the static horizontal load test as well as dynamic horizontal load test was performed on the permanent foundation piles which had a pile length of 30 m, 800 mm in outer diameter and 15 mm in wall thickness. In this site the dynamic horizontal load test on a smaller test pile, 12 m in length, 500 mm in outer diameter and 12 mm in wall thickness, was also carried out.

In this paper, first the results of static and dynamic horizontal load tests on the permanent foundation piles are presented and compared. Then the horizontal load displacement of the permanent foundation pile is predicted based on the results of the dynamic horizontal load test of the smaller diameter pile. The predicted results are compared with the measured results, and discussions will be made.

PILE LOAD TEST

Test site and test pile

A bridge was constructed at the Kiusu site for the Central Hokkaido Connection Road in 2005. A pile group foundation was employed for an abutment of the bridge. A total of 40 steel pipe piles with a centre to centre distance of 2.2 m and 3.0 m were driven by a hydraulic hammer (see Fig. 1).

In order to assess the performance of the constructed piles in the site and to obtain design parameters for piles in the future, a static alternating cyclic horizontal load test and a dynamic horizontal load test were carried out on the constructed foundation piles H35 and H36, respectively. Moreover, with an aim to predict the horizontal load displacement of the actual pile from the load test of a test pile which had smaller sizes than those of the actual pile, dynamic horizontal load test was conducted on the test pile T01 which was located 5 m away from the pile H36 as shown in Fig. 1. The specifications of both the test pile and the actual piles are summarised in Table 1.

Fig. 2 shows the profiles of soil layers and SPT *N*-values at Kiusu site. The soil profile at this site is characterised by thick deposits of volcanic soils. SPT *N*-values are typically less than 7, except for gravel at depths from 17.5 m to 21.2 m and volcanic soils at depths from 27.5 m to 31 m. No definite bearing stratum having *N*-values greaten than 30 can be found to a depth of 32 m.

Test method and test procedure

Prior to the dynamic horizontal load tests, static alternating cyclic horizontal load test was carried out on the pile H35. Details of the static alternating cyclic horizontal load test can be found in Tomisawa et al. (2006).

In the dynamic horizontal load test, the pile was hit horizontally by a hammer mass of 2.14 ton through a coil spring which was attached to the load cell at the point z = 0.3 m below the pile head as shown in Photo 1 and Fig. 3.

Applied force, horizontal displacements and accelerations were measured at the same level of the hit point with a sampling interval of 15 ms. Details of the loading and measuring devices are shown in Fig. 3. The measuring devices and their frequency characteristics are listed in Table 2.

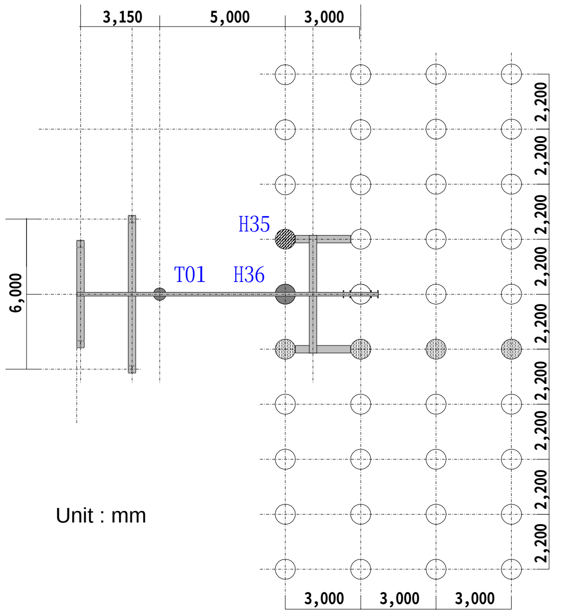

Fig. 1. Arrangement of piles at the test site.

Table 1. Specifications of test and actual piles.

	T01	H35&H36
Length (m)	12.0	30.0
Embedment length (m)	11.2	29.2
Outer diameter (mm)	500	800
Inner diameter (mm)	476	770 * 782 **
Cross-sectional area (cm^2)	184.0	369.2 * 223.7 **
Young's modulus (kN/m^2)	2.06×10^8	2.06×10^8
Bending rigidity (cm^2)	1.13×10^5	5.87×10^5 3.60×10^5
Shear wave velocity (m/s)	3187	3187
Density (ton/m^3)	7.8	7.8
Mass (ton)	1.7	5.9

* Upper part (z < 6 m), ** Lower part (z > 6 m)

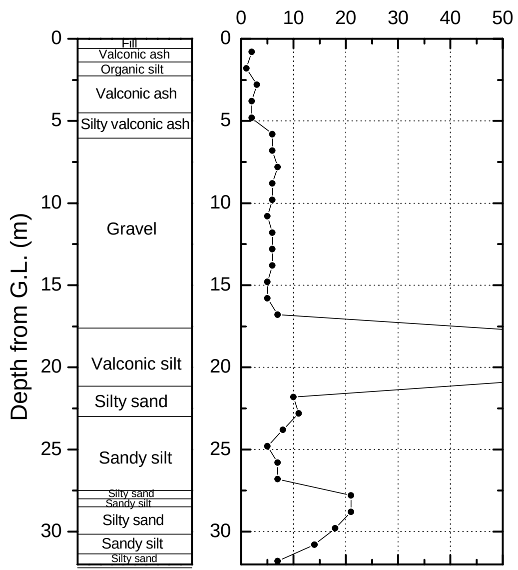

Fig. 2. Profiles of soil layers and SPT *N*-values.

Table 2. Frequency characteristics of measuring devices.

		Frequency characteristic
Sensor	axial strain gauge	DC ~ 300 kHz
	accelerometer	0.7 Hz ~ 10.0 kHz
	load cell	DC ~ 1.7 kHz
	displacement transducer	DC ~ 20.0 Hz
Amplifier	axial strain gauge	0.1 Hz ~ 6.0 kHz
	accelerometer	DC ~ 10.0 kHz
	load cell	DC ~ 2.5 kHz
	displacement transducer	DC ~ 2.5 kHz

Photo 1. Loading and measuring devices in the Kiusu site.

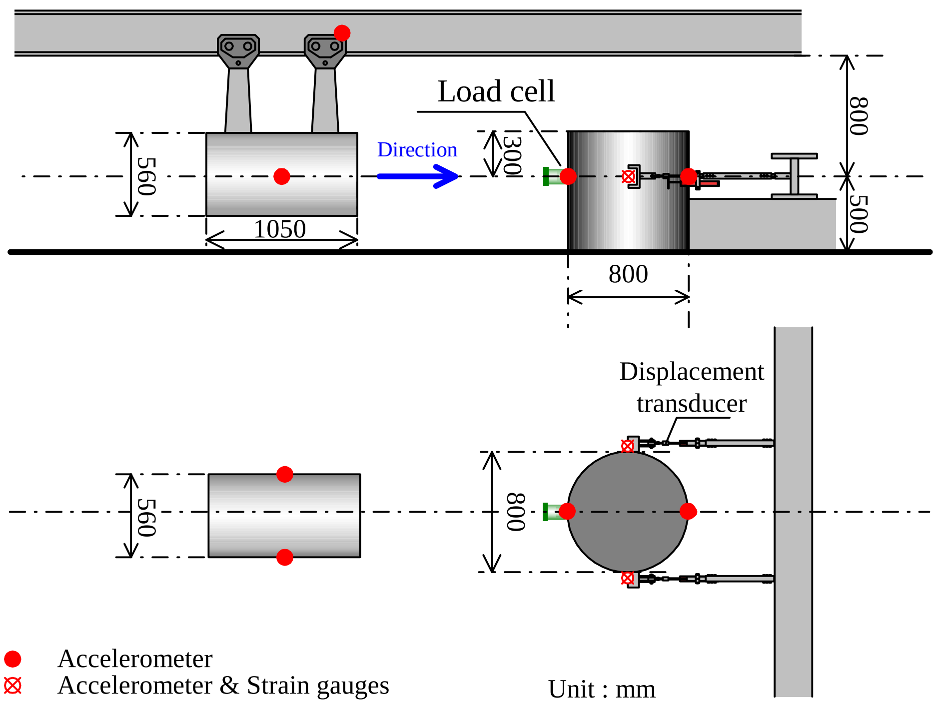

Fig. 3. Loading and measuring devices for dynamic horizontal load test.

Test results

Fig. 4 shows the relationships between the static horizontal load and the horizontal displacement of the pile H35. The residual displacement was measured at full recovery of horizontal load to 0 in each load step, and the elastic displacement was obtained by subtracting the residual displacement from the total displacement measured at the maximum load in each load step. The residual displacement and the corresponding elastic displacement for at the maximum load in each load step are also shown in Fig. 4.

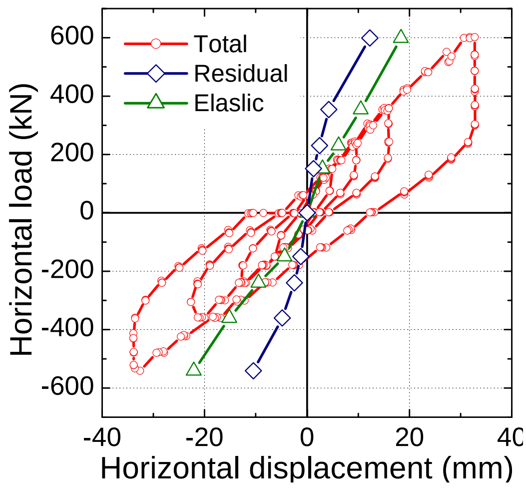

Fig. 4. Static horizontal load vs displacement.

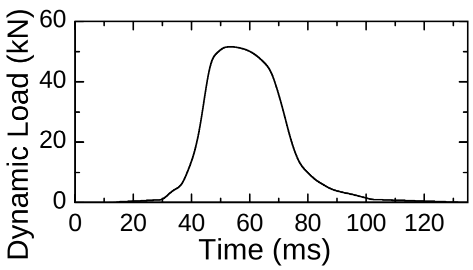

(a) Measured dynamic load

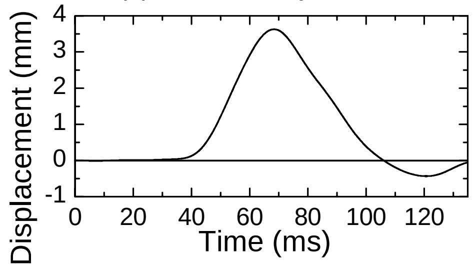

(b) Measured displacement

Fig. 5. Measured dynamic pile load test signal.

An example of the dynamic test signals of the pile H36 are shown in Fig. 5. The measured force increases and decreases smoothly with time, and has a peak of about 50 kN. The loading duration is about 70 ms. The measured displacement also increases and decreases with time having a peak of 3.6 mm at a time of 68 ms. The peak horizontal displacement delays 16 ms behind the peak horizontal load, showing dynamic effects. A total of eight dynamic load tests were carried out on the pile H36.

The axial strains measured at different depths down the pile shaft are shown in Fig 6. It can be seen from the figure that only the upper part of the pile (< G.L. -8.2 m) deforms during the dynamic horizontal load test.

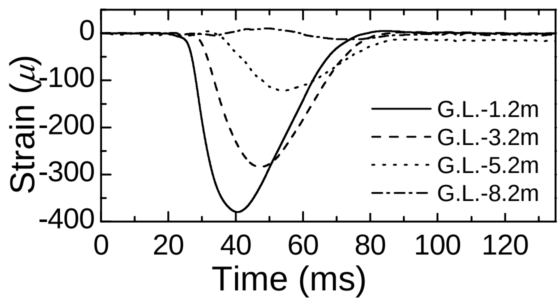

Fig. 6. Measured strain at different depths.

Fig. 7 shows the relationships between the dynamic horizontal load and the horizontal displacement. It can be seen from comparison between Fig. 4 and Fig. 7 that the measured load displacement relations from the dynamic load tests are totally different from the measured static load displacement relations. Therefore, in order to obtain the static load displacement relation of the pile from the measured signals of the dynamic load test, wave matching analysis of the measured dynamic signals is needed.

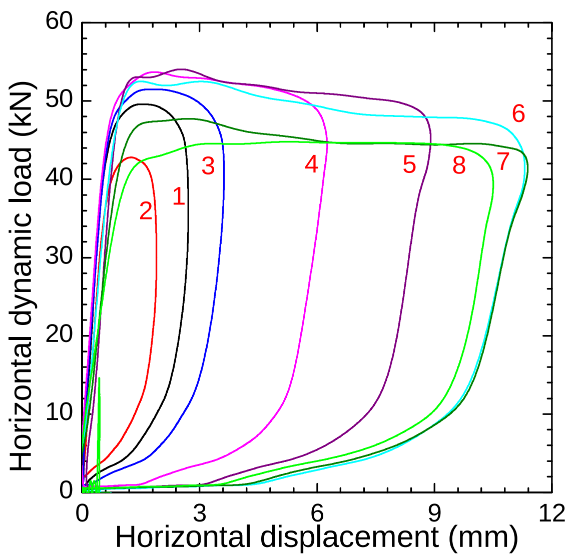

Fig. 7. Measured dynamic load displacement.

ANALYSES OF TEST RESULTS

A computer program KWaveHybrid, developed by Kitiyodom et al. (2006), was used for the wave matching analysis of the dynamic horizontal load test. The program was also used to estimate the static load displacement relationship of the pile using the soil parameters obtained from wave matching analysis.

Fig. 8 illustrates the hybrid modelling of the pile and the soil used in KWaveHybrid. The pile is modeled as beam elements with masses and the soil is treated as springs and dashpots.

Fig. 9 shows the dynamic shaft soil resistance model proposed by Randolph and Deeks (1992) for vertical shaft resistance. This model was incorporated into KWaveHybrid for both vertical and horizontal resistances at the pile shaft nodes. The values of the vertical spring, k, the horizontal springs, k^x and k^y, the vertical radiation damping, c, and the horizontal radiation damping, c^x and c^y, per unit shaft area are approximated by means of Eqs. 1 and 2, based on the work of Novak et al. (1978).

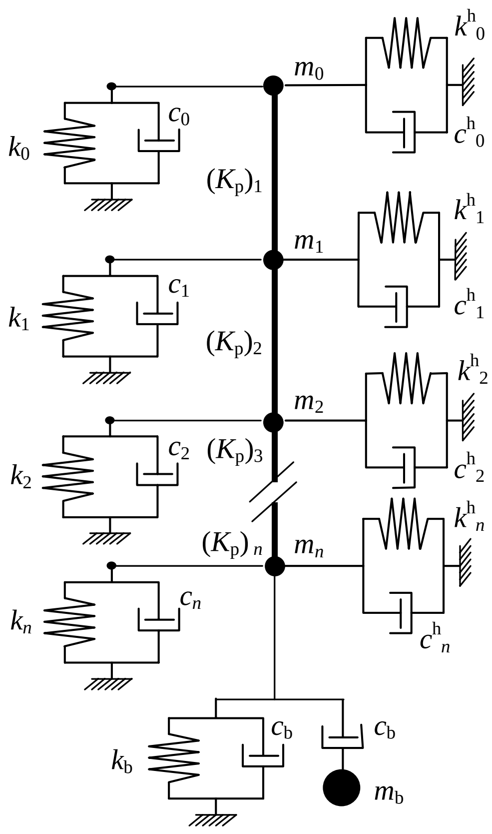

Fig. 8. Hybrid modelling of the pile and the soil.

$$k = \frac{2.75G_s}{\pi d},\ k^x = k^y = \frac{4G_s}{d} \quad (1)$$

$$c = \frac{G_s}{V_s},\ c^x = c^y = \frac{4.5G_s}{V_s} \quad (2)$$

where G_s and V_s are the shear modulus and the shear wave velocity of the surrounding soil respectively, and d is the outer diameter of the pile.

The slider value is equal to the static maximum shaft resistance in the vertical direction and is equal to the limit horizontal pressure in the horizontal direction.

Fig. 10 shows the dynamic vertical pile base resistance model. The values of the soil spring at the pile base, k_b, the damping, c_b, and the lumped soil mass, m_b, per unit base area can be estimated as follows (Randolph and Deeks, 1992):

$$k_b = \frac{8G_s}{\pi d(1-\nu_s)} \quad (3)$$

$$c_b = \frac{3.4}{\pi(1-\nu_s)}\frac{G_s}{V_s} \quad (4)$$

$$m_b = 16 r_o \rho_s \frac{0.1-\nu_s^4}{\pi(1-\nu_s)} \quad (5)$$

in which ν_s and ρ_s are the Poisson's ratio and the density of the soil, respectively.

In the analysis of static pile load test, the static vertical shaft soil spring, k_{static}, is estimated by means of Eqs. 6 and 7 following Randolph and Wroth (1978).

$$k_{static} = (2\pi / 2.75\xi)\cdot k\ ,\ \xi = \ln[5.0(1-\nu_s)L/d] \quad (6)$$

where L is the pile embedment length.

The static horizontal shaft soil spring values at each pile node are estimated based on Mindlin's solution (Mindlin, 1936) which is similar to the solution of the integral equation method used by Poulos and Davis (1980). The equations become

$$k^x_{static} = k^y_{static} = \zeta E_s \Delta L \quad (7)$$

$$\zeta = pd / uE_s \quad (8)$$

where *p* is the horizontal distributed force acting uniformly over the pile element and *u* is the corresponding horizontal displacement at each pile node calculated using the integral equation method. More details of the analysis method can be found in Kitiyodom et al. (2006)

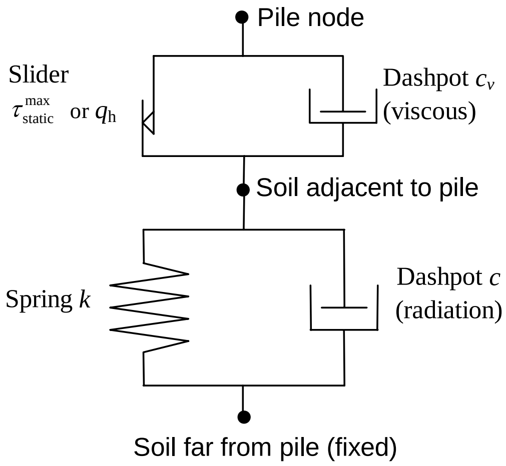

Fig. 9. Vertical and horizontal shaft resistance model.

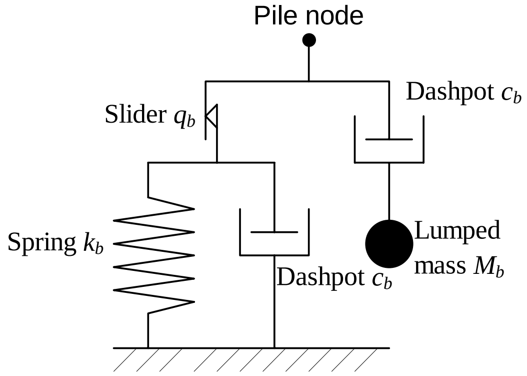

Fig. 10. Vertical base resistance model.

It should be noted here that the unloading and reloading curves measured in the static alternating cyclic load test (Fig. 4) indicate that gapping between the pile and the surround soil occurs during unloading and reloading stages. Such gapping has not been incorporated in KWaveHybrid at present. Hence, monotonic horizontal loading of the pile is considered in the analysis. Note also that the interiors of the pipe piles were almost filled with soil at the end of driving. However, the masses of the soil inside the pipe piles were not taken into account in the analyses.

Analysis results of the actual pile H36

Matching analysis was repeated with assumed values for the maximum shaft horizontal pressure, q_h, and the soil shear modulus, G_s, using the measured dynamic load (Fig. 11) as the force boundary condition at the loading point, until a good matching between the calculated and the measured pile displacements was obtained. Soil parameters used in the final matching of the pile H36 are listed in Table 3. Fig. 12 and Fig. 13 show the displacement versus time and load versus displacement of the pile H36 calculated in the final matching analysis, compared with the measured values.

It can be seen that the calculated dynamic pile displacement overestimated the measured values after the peak displacement. This is thought to be due to the soil spring model. At the present, the values of the soil spring in KWaveHybrid during the loading and unloading states are the same. The values of the soil spring during the loading and unloading states should be different due to gapping between the pile and the surrounding soil as mentioned earlier. However, the calculated displacement matches very well with the measured displacement until the peak displacement.

Table 3. Soil parameters identified in final matching of H36.

Depth (m)	G_s (kPa)	ν_s	q_h (kPa)
0 to 3.6	7692	0.3	8.1
3.6 to 15.6	9231	0.3	Elastic range
> 15.6	53846	0.3	Elastic range

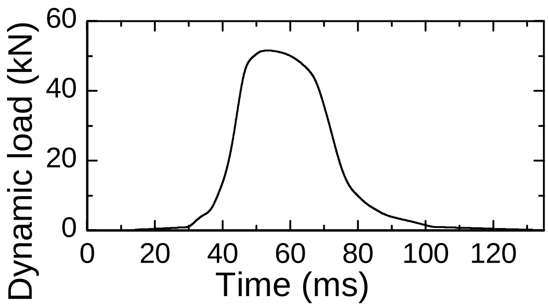

Fig. 11. Measured dynamic load of H36.

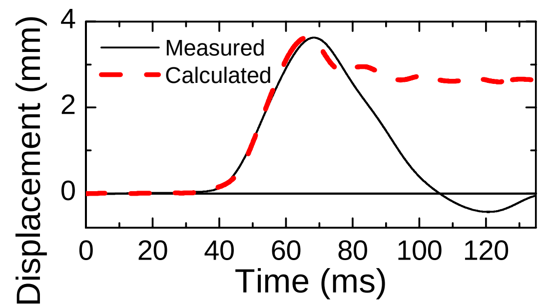

Fig. 12. Measured and calculated displacement of H36.

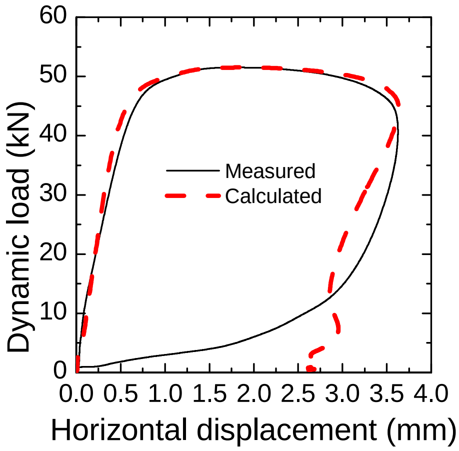

Fig. 13. Measured and calculated load-displacement of H36.

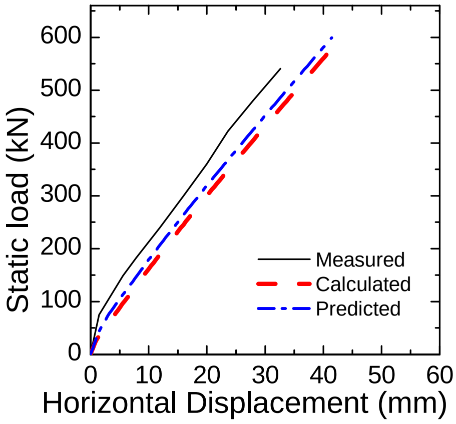

Fig. 14. Measured, calculated and predicted static load displacement of H36.

Using the same soil parameters as shown in Table 3, the static load displacement relation of the pile H36 was estimated using KWaveHybrid. Fig. 14 shows the comparison of the calculated static load displacement relation with the measured value. It can be seen that the calculated result matches well with the measured one.

Analysis results of the test pile T01

The same analysis procedures as used for the pile H36 were carried out for the test pile T01. Soil parameters used in the final matching of the pile T01 are listed in Table 4. The measured dynamic load versus time is shown in Fig 15. Fig. 16 and Fig. 17 show the displacement versus time and load versus displacement of the pile T01 calculated in the final matching analysis, compared with the measured values.

Fig. 18 shows the static horizontal load versus horizontal displacement of the pile T01 derived from the dynamic horizontal load test.

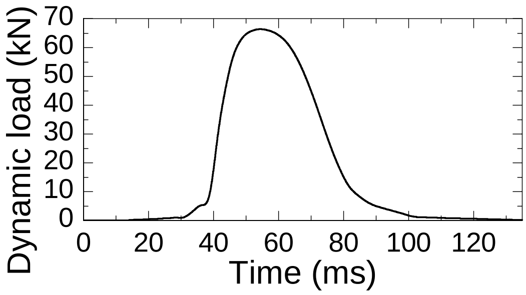

Fig. 15. Measured force of T01.

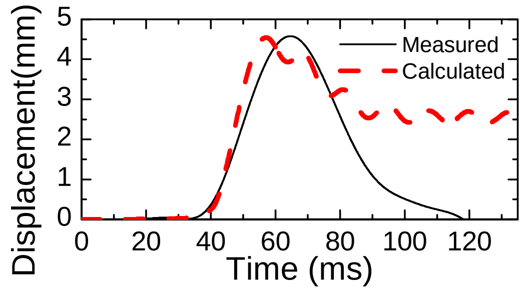

Fig. 16. Measured and calculated displacement of T01.

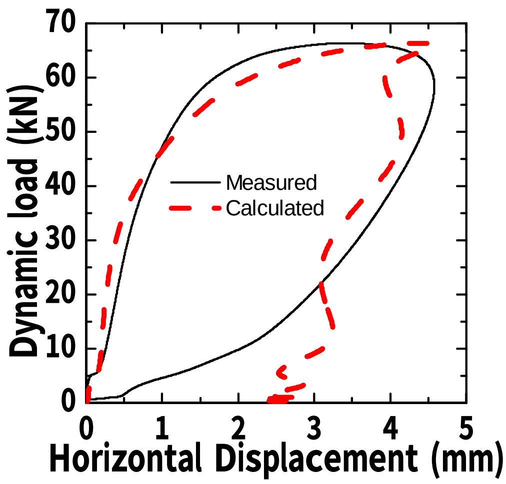

Fig. 17. Measured and calculated load-displacement of T01.

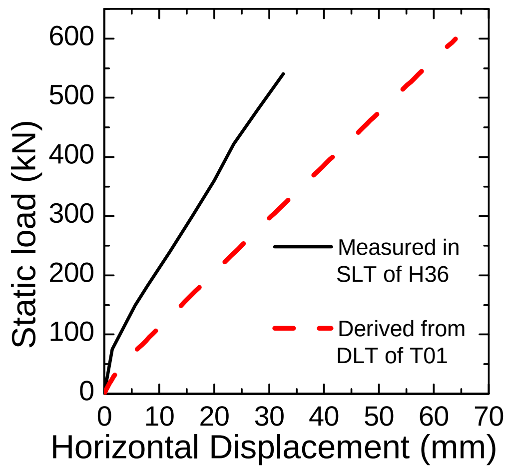

Fig. 18. Comparison of static load-displacement between H36 and T01.

Table 4. Soil parameters identified in final matching of T01.

Depth (m)	G_s (kPa)	ν_s	q_h (kPa)
0 to 3.6	7692	0.3	23.0
3.6 to 15.6	9231	0.3	Elastic range
> 15.6	53846	0.3	Elastic range

For comparison purpose, the measured static horizontal load versus horizontal displacement of the pile H36 is also shown in the figure. As expected, the horizontal stiffness of the smaller test pile T01 is lower than that of the actual constructed pile H36.

PREDICTION ANALYSIS

In actual construction site, it would be very useful to estimate the static load displacement relation of the actual pile from the dynamic load test of another pile having smaller sizes. The soil parameters of the pile T01 (Table 4), which has a smaller size than the pile H36, were employed to predict the load displacement relation of H36.

Fig. 19 and Fig. 20 show the predicted displacement vs time and the predicted dynamic load displacement relation of H36, compared with the measured values, respectively. It can be seen that the predicted pile displacements considerably underestimate the measured values.

The static load displacement relation of H36 derived from the prediction analysis has been indicated in Fig. 14. It can be seen that the predicted result matches well with the measured one, although good matching for the dynamic signals was not obtained. Further study will be needed to use the test pile having different configurations from the actual pile for predicting the performance of the actual pile.

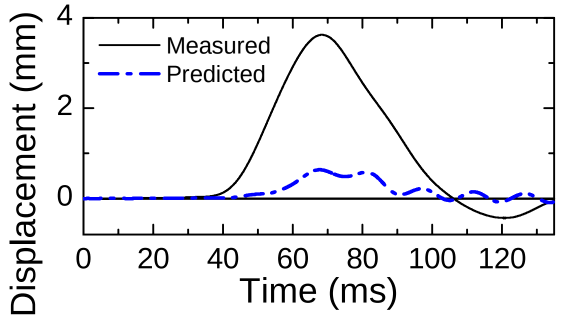

Fig. 19. Measured and predicted displacements of H36.

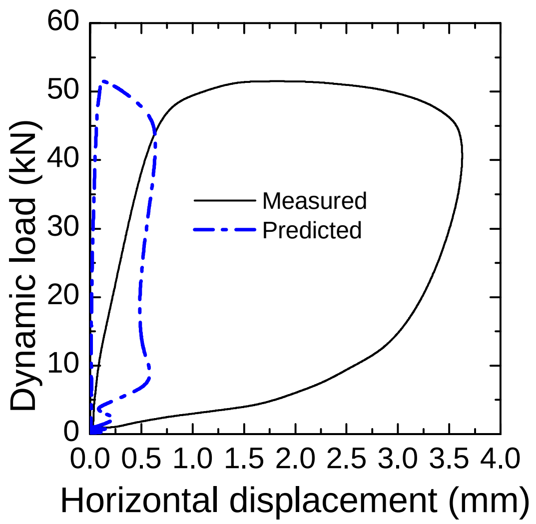

Fig. 20. Measured and calculated load-displacement of T01.

CONCLUSIONS

In this paper, the results of alternating cyclic horizontal load tests and dynamic horizontal pile load tests on driven open-ended steel pipe piles constructed for foundations of a bridge abutment at Kiusu site have been presented and discussed

A good matching between the calculated and measured behaviours of the piles during driving and during static load test was obtained.

The possibility of the use of dynamic horizontal pile load test as an alternative method for the conventional static horizontal load testing was demonstrated.

REFERENCES

Kitiyodom, P., Matsumoto, T., Kojima, E., Kumagai, H. and Tomisawa, K., 2006. Analysis of static and dynamic horizontal load tests on steel pipe piles. *Proceedings of 10th International Conference on Piling and Deep Foundations*, Amsterdam (to be published).

Mindlin, R. D., 1936. Force at a point interior of a semi-infinite solid. *Physics*, 7, 195-202.

Poulos, H. G. and Davis E. H., 1980. *Pile Foundation Analysis and Design*, Wiley, New York.

Novak, M., Nogami, T. and Aboul-Ella F., 1978. Dynamic soil reactions for plane strain case. *Journal of Mechanical Engineering ASCE*, 104(EM4), 953-959.

Randolph, M. F. and Deeks A. J., 1992. Dynamic and static soil models for axial pile response. Proceedings of 4th International Conference on the Application of Stress-Wave Theory to Piles, The Hague, 3-14.

Randolph, M. F. and Wroth, C. P., 1978. Analysis of deformation of vertically loaded piles. *Journal of Geotechnical Engineering ASCE*, 104(12), 1468-1488.

Tomisawa, K., Nishimoto, S., Fukushima, H., Saitoh, A., Kojima, E. and Matsumoto, T., 2006. Static alternating cyclic horizontal load test on a driven steel pipe pile in the foundation for a highway bridge. *Proceedings of 10th International Conference on Piling and Deep Foundations*, Amsterdam (accepted for publication).